Sensitized Near-IR Luminescence of Ln(III) Complexes with Benzothiazole Derivatives

Min-Kook Nah,[†,‡] Soo-Gyun Rho,[†] Hwan Kyu Kim,*[,†,§] and Jun-Gill Kang*[,‡]

Center for Smart Light-Harvesting Materials and Department of Advanced Materials, Hannam University, Deajeon 306-791, and Department of Chemistry, Chungnam National University, Daejeon 304-764, Korea

Received: July 11, 2007; In Final Form: August 22, 2007

Lanthanide complexes with benzothiazole derivatives (Btz-R, R = OCH_3 and OH) and terpyridine (tpy) ligands were synthesized, and their photophysical properties were precisely investigated. The free Btz-OCH_3 ligand in toluene, excited with UV light, produced the normal emission bands around 410 nm, whereas Btz-OH produced a strong excited-state intramolecular proton transfer (ESIPT) band at 510 nm. The Ln(III) complexes (Ln = Nd, Er, and Yb) exhibited sensitized near-IR luminescence when the Btz-R ligands were excited. The sensitized luminescence quantum yields (Φ_{Ln}) of the lanthanide complexes were markedly enhanced by ESIPT: for [Nd(Btz-R)(tpy)] in toluene solution, Φ_{Ln} = 0.04% for Btz-OCH_3 and 0.39% for Btz-OH. The sensitized luminescence of the Er(III) complexes (Φ_{Ln} = 0.002% for Btz-OCH_3 and 0.009% for Btz-OH) was less efficient than that of the Nd(III) complexes. This difference is due to the smaller energy gap between the emitting and ground levels of the Er(III) ion. The rate constants for the energy transfer from Btz-R to Ln(III) were about $\sim 10^9$ s^{-1}, as evaluated by the Förster resonance energy transfer mechanism.

Introduction

The lanthanide ions have attracted great attention because of their widely applicable potential in generating and amplifying laser light and their roles in light-emitting diodes (LEDs), medical applications (immunoassay, MRI contrast reagent), chemical sensors, and optical communications.[1−3] Notably, lanthanide ions, such as Nd(III), Er(III), and Yb(III), which emit in the near-infrared (NIR), have been incorporated into silica optical fibers for the optical signal amplifiers of telecommunication network system. However, the limited solubility of lanthanide ions in conventional inorganic/organic media has resulted in poor amplification. Instead of dopants, NIR-luminescent lanthanide complexes with organic ligands hold promise for application in telecommunication devices. In general, however, the f → f absorption cross-sections of lanthanide ions are very small. In an effort to obtain highly efficient luminescence from lanthanide complexes, the ligand-containing chromophore has been introduced as an antenna to the lanthanide complex. In this system, intramolecular energy transfer takes place from the organic antenna molecules to the localized intra-4f shell of the lanthanide ion, resulting in luminescence with an enhanced quantum yield. Typical chromophores used as antennas are phenanthroline,[4−7] anthracene,[8−10] terphenyl,[4,11] calixarenes,[12] and podands.[13−15]

Benzothiazole derivatives, including hydroxyphenyl, exhibit excited-state intramolecular proton transfer (ESIPT), which often involves a large Stokes shift. This phenomenon has widespread implications in UV light stabilizers,[16] laser dyes,[17] new polymeric materials,[18,19] and fluorescence probes for labeling proteins.[20] In the ESIPT mechanism, the UV light absorption through the *cis*-enol produces the excited *cis*-enol, which is quickly converted to an excited keto tautomer by intramolecular proton transfer. During this process, the hydrogen becomes more acidic and the nitrogen becomes more basic in the excite state.[21] The ESIPT mechanism is dependent on the solvent polarity.[22−24] Changes in the spectral distribution of ligand molecules may be related to changes in the energy transfer efficiency. The energy transfer process from the benzothiazole derivatives to central lanthanide ions has not yet been reported. Especially, the effect on NIR luminescence owing to functional groups such as −OH and −OCH_3 attached to benzothiazole derivatives has not been determined. In this paper, we report the preparation of suitable NIR-emitting Ln(III) complexes with benzothiazole derivatives, including methoxybenzoic or hydroxybenzoic acid groups, and their optical properties in various solvents. We also demonstrate an ESIPT effect on the sensitized NIR luminescence of lanthanide ions and discuss the energy transfer mechanism in relation to the resonance energy transfer mechanism.

Experimental Methods

Synthesis. The benzothiazole derivatives (Btz-R, R = OCH_3 and OH) and their Ln(III) complexes were synthesized as follows. The flame-dried Schlenk flask was charged with a mixture of Btz-R (0.54 mmol), terpyridine (0.18 mmol), and KH (0.64 mmol) in a glovebox. Next, 100 mL of dried THF was transferred to the Schlenk flask through a cannula, and the solution was stirred at room temperature overnight. The reaction proceeded with gas evolution, and a solution of anhydrous $LnCl_3$ (0.18 mmol) in 10 mL of methanol was added to the reaction solution. After 2 days of stirring at room temperature, the solution had produced a white precipitate. The precipitate was washed with methanol and diethyl ether to give [Ln(Btz-R)$_3$-(tpy)], where R = OCH_3 and OH and tpy = terpyridine, as a white solid (Scheme 1).

Photophysical Measurements. The UV−vis spectra of free Btz-R and their Ln(III) complexes dissolved in various solvents were recorded at room temperature in a quartz cell with a 1 cm path length on a Shimadzu UV-2401PC spectrophotometer. The

* To whom correspondence should be addressed. (H.K.K.) E-mail: hkk777@korea.ac.kr. Phone: +82-41-860-1493. Fax: +82-41-867-5396. (J.-G.K.) E-mail: jgkang@cnu.ac.kr. Phone: +82-42-821-6548. Fax: +82-42-821-8896.

† Hannam University.

‡ Chungnam National University.

§ Current address: Department of Chemistry, Korea University, Jochiwon, Chungnam 339-700, Korea.

10.1021/jp0753979 CCC: $37.00
Published on Web 10/18/2007

SCHEME 1

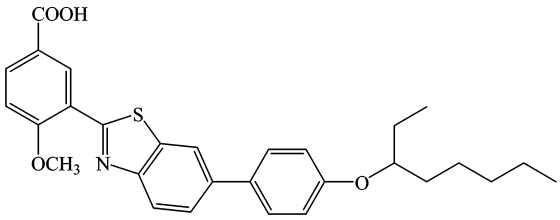

3-{6-[4-(1-Ethyl-hexyloxy)-phenyl]-benzothiazol-2-yl}-4-methoxy-benzoic acid

(Btz-OCH$_3$)

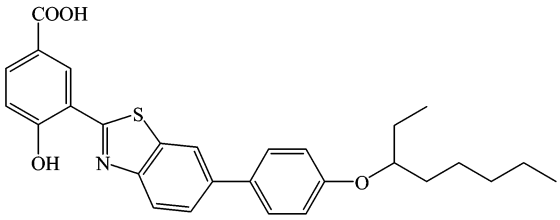

3-{6-[4-(1-Ethyl-hexyloxy)-phenyl]-benzothiazol-2-yl}-4-hydroxy-benzoic acid

(Btz-OH)

excitation and luminescence spectra of free Btz-R and their Ln-(III) complexes were measured on a steady-state fluorospectrometer (Edinburgh Instruments FS920) equipped with a 450 W Xe lamp. The luminescence spectra in the visible region were recorded with a PMT system (Hamamatsu R955), and the luminescence spectra in the NIR region were recorded with a Ge detector (Edinburgh Instruments EI-L) cooled by liquid nitrogen.

The quantum yield of the visible luminescence for each sample (Φ_s) was determined by the relative comparison procedure, using a reference of a known quantum yield (quinine sulfate in diluted H_2SO_4 solution, $\Phi_r = 0.546$). The general equation used in the determination of the relative quantum yield is as follows:[25]

$$\Phi_s = \Phi_r\left(\frac{A_r(\lambda_r)}{A_s(\lambda_s)}\right)\left(\frac{I(\lambda_r)}{I(\lambda_s)}\right)\left(\frac{n_s^2}{n_r^2}\right)\left(\frac{D_s}{D_r}\right) \quad (1)$$

where $A(\lambda)$ is the absorbance, $I(\lambda)$ is the relative intensity of the exciting light at wavelength λ, n is the average refractive index of the solvent, and D is the integrated area under the corrected emission spectrum.

For the measurements of the decay time in the visible region, a time-correlated single photon counting (TCSPC) method was employed. The excitation source was a self-mode-locked Ti−sapphire laser (Coherent model Mira 900) pumped by a Nd:YVO_4 laser (Coherent Verdi diode-pumped laser). The laser output has a ∼200 fs pulse width with a repetition rate of 76 MHz and spanned the excitation wavelength in the range of 350−490 nm by a second-harmonic generation. All the standard electronics for the TCSPC system were from Edinburgh Instruments. The instrument function was measured by detecting the scattered laser pulse of ∼200 fs with a quartz crystal. The resultant FWHM is 3 ps. For measurements of the decay times in the NIR region, a high-power ns-Nd:YAG laser system was used with a pump wavelength selected within the third-harmonic generation. The laser output had a pulse width of ∼5 ns with a repetition rate of 10 Hz. The final pump laser pulse was adjusted to a wavelength of 416 nm using a hydrogen gas-filled Raman shifter. The electric output signals were collected with a digital oscilloscope system (Agilent Infiniium 54832B). All samples were diluted in either toluene or ethanol for spectroscopic measurement, and the concentrations were adjusted to approximately 10^{-5} M.

Theoretical Models

Judd−Ofelt Intensity Parameters. Judd−Ofelt theory[26,27] has been very successful in explaining and predicting the spectral intensities of the induced electric dipole transitions, especially for the absorption spectrum of lanthanide ion. According to the Judd−Ofelt theorem, the oscillator strength of an electric dipole transition from the initial state to the final state (P^{ed}) is expressed by

$$P^{ed} = \frac{8\pi^2 mc}{3h}\frac{\nu_P}{2J+1}\frac{(n^2+2)^2}{9n}\sum_{\lambda=2,4,6}\Omega_\lambda|\langle\alpha' J'||U^{(\lambda)}||\alpha J\rangle|^2 \quad (2)$$

where ν_P is the center of the absorption transition (cm^{-1}), $|\langle||U^{(\lambda)}||\rangle|^2$ represents the square of the matrix elements of the unit tensor operation $U^{(\lambda)}$ ($\lambda = 2$, 4, and 6)[28] connecting the initial and final states, and the Ω_λ values ($\lambda = 2$, 4, and 6) are Judd−Ofelt intensity parameters. In eq 2, the Judd−Ofelt parameters are strongly dependent on the ligand environment, as the matrix elements of the unit tensor operators between two energy manifolds in a given lanthanide ion are for the free ion state.[29,30] Experimentally, the oscillator strength is related to the integrated area in the absorption band and can be expressed in terms of the extinction coefficient $\epsilon(\nu)$ and the energy of the transition ν (cm^{-1}) according to[26,27,31]

$$P_{exp} = (4.3218 \times 10^{-9})\frac{1}{Cl}\int \mathrm{Abs}(\nu)\,\mathrm{d}\nu \quad (3)$$

where $\mathrm{Abs}(\nu)$ is the optical density as a function of ν, l is the thickness of the solution sample, and C is the concentration of

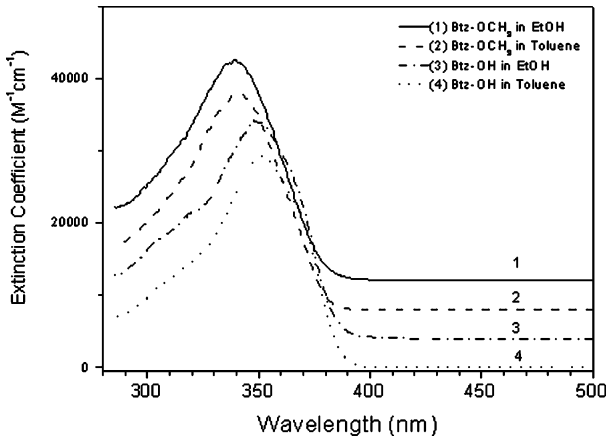

Figure 1. Absorption spectra of Btz-R (R = OCH_3 and OH) ligands in toluene and ethanol.

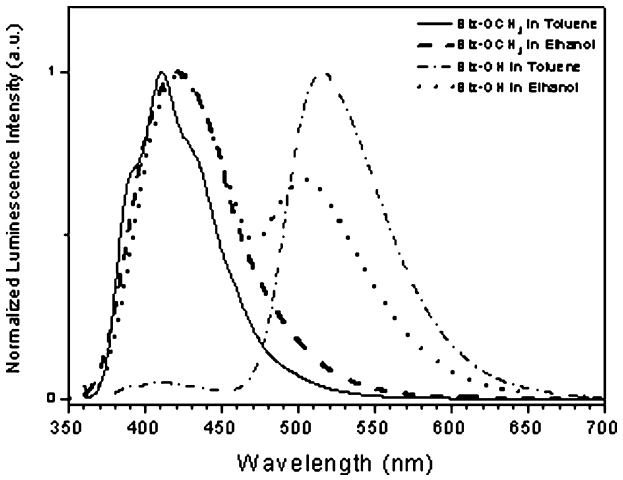

Figure 2. Luminescence spectra of Btz-R (R = OCH_3 and OH) ligands in toluene and ethanol (λ_{ex} = 345 nm).

lanthanide ions (mol/L). The Judd−Ofelt parameters can be obtained from eqs 2 and 3.

Energy Transfer Rate. In general, the dipole−dipole (dd), dipole−multipole (mp), and resonance transfer mechanisms have been considered for the energy transfer from an organic ligand to a lanthanide ion. Previously, we reported these mechanisms for Er(III) complexes with platinum 5,10,15-triphenyl-20-(4-carboxyphenyl)porphyrin (PtP) and tpy ligands in an organic solution.[32] Modeling the results on the dd and md mechanisms produced unreasonably small rate constants, whereas the Förster resonance energy transfer mechanism correctly explained the energy transfer rate constants. Similarly, the Förster mechanism more reliably accounted for the sensitized NIR luminescence of Ln(III) in the solution state. The energy transfer rate k_{ET}^{res} for the Förster mechanism can be expressed by[33]

$$k_{ET}^{res} = \frac{1}{\tau_D}\left(\frac{R_0}{R_L}\right)^6 \quad (4)$$

where τ_D is the decay time of the donor in the absence of an acceptor. In eq 4, R_0 is the critical distance (Å), which is expressed by

$$R_0 = 0.211[\kappa^2 n^{-4} \Phi_D \int F_D(\lambda)\, \epsilon_A(\lambda)\, \lambda^4\, d\lambda]^{1/6} \quad (5)$$

In eq 5, κ^2 describes the relative orientation in space of the transition dipoles of the donor and acceptor and is usually assumed to be equal to 2/3, n is the refractive index of the medium, and Φ_D is the quantum yield of the donor in the absence of an acceptor. The integral function describes the spectral overlap integral, which can be calculated by

$$J = \int F_D(\lambda)\, \epsilon_A(\lambda)\, \lambda^4\, d\lambda \quad (6)$$

The integral covers the normalized emission band shape of the sensitizer $F_D(\lambda)$ and the normalized absorption band of the acceptor $\epsilon_A(\lambda)$.

Results and Discussion

Photophysical Properties of Btz-R Ligands. Figure 1 shows the absorption spectra of Btz-R (R = OCH_3 and OH) dissolved in toluene and ethanol, respectively. Similar absorption spectra were observed for both Btz-OCH_3 and Btz-OH, with absorption maxima around 340 nm for Btz-OCH_3 and 350 nm for Btz-OH and with extinction coefficients of approximately 30 000 M^{-1} cm^{-1}. The luminescence and excitation spectra of Btz-OCH_3 and Btz-OH dissolved in ethanol and toluene were also measured. As shown in Figure 2, the luminescence spectra of Btz-OCH_3 were almost identical in both solvents, with maxima at 420 nm and with excitation bands that resembled the absorption bands. In contrast, the luminescence spectrum of Btz-OH varied with the solvent. As shown in Figure 3, Btz-OH in ethanol produced two emission bands, with maxima at 420 and 510 nm, where the 420 and 510 nm bands can be assigned as the normal and ESIPT luminescence, respectively. In ethanol, the intensity of the normal band was stronger than that of the ESIPT band. In toluene, the intensity of the ESIPT band was notably strong, whereas the intensity of the normal band was decreased, appearing as only a trace. The excitation spectra of the low-energy and high-energy emission bands of Btz-OH were similar to those of Btz-OCH_3. Additionally, the Stokes shift of the low-energy band was very large, greater than 100 nm. These results demonstrate that the Btz-OH molecule undergoes ESIPT more effectively in toluene than in ethanol.[34−36] In ethanol, some part of the Btz-OH molecules might form intermolecular hydrogen bonds with the solvent, preventing the Btz-OH molecule from undergoing ESIPT. The relative intensities of the normal and ESIPT bands suggest that intermolecular hydrogen bonding is more favorable than ESIPT in ethanol.

Photophysical Properties of Ln(III) Complexes. *Absorption*. The absorption spectra of [Ln(Btz-R)$_3$(tpy)] (R = OCH_3 and OH) were also measured in toluene and ethanol. The absorption spectra were very similar to those of the free Btz-R ligands. The concentration of 1.0×10^{-5} M was too low to produce the characteristic transitions of lanthanide ions or the ligand tpy. The measurements indicate that the light was primarily absorbed by Btz-R (R = OCH_3 and OH) ligands and that the direct excitation of the lanthanide ion was limited at the 1.0×10^{-5} M concentration.

The Judd−Ofelt intensity parameters were calculated to investigate the influence of the ligands on the complexation of the lanthanide ion, using Nd(III) complexes and a concentration of 1.0×10^{-2} M. The five absorption bands distinctively observed in the visible region had observed barycenters of 13 477, 14 683, 15 810, 17 130, and 18 981 cm^{-1}, attributable to the $^4I_{9/2} \rightarrow \{^4S_{3/2}, ^4F_{7/2}\}$, $\{^4F_{9/2}\}$, $\{^2H_{11/2}\}$, $\{^2G_{7/2}, ^4G_{5/2}\}$, and $\{^4G_{9/2}, ^4G_{7/2}, ^2K_{13/2}\}$ transitions, respectively.[28] Applying eqs 2 and 3 to the observed bands, followed by the integration of the resolved bands, we evaluated the Judd−Ofelt intensity parameters (Ω_λ, λ = 2, 4, and 6). Among the Judd−Ofelt intensity parameters, Ω_2 is sensitive to the ligand environment, when the value of the matrix element $U^{(2)}$ is comparable to the values of $U^{(4)}$ and $U^{(6)}$. Hypersensitivity was observed in the $^4I_{9/2} \rightarrow$

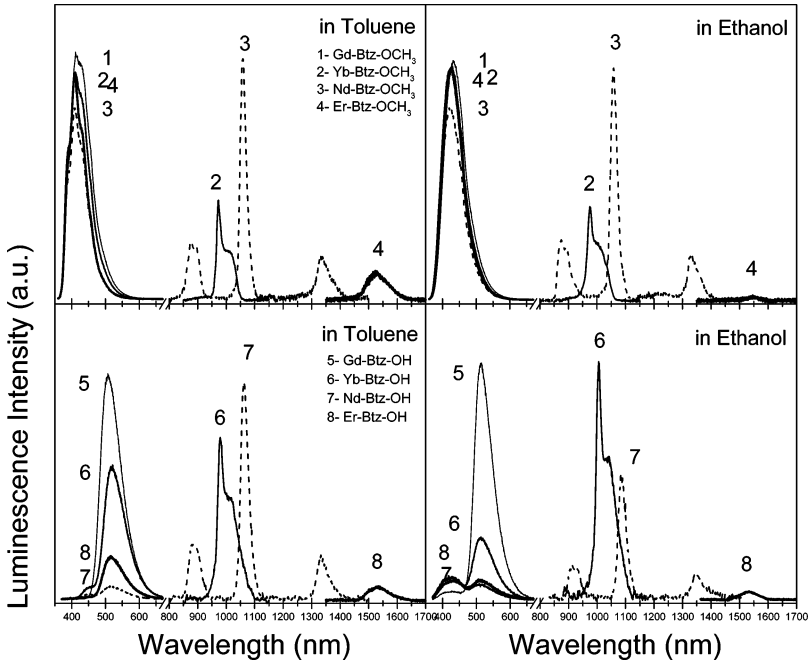

Figure 3. Luminescence spectra of [Ln(Btz-OCH_3)$_3$(tpy)] (λ_{ex} = 345 nm) and [Ln(Btz-OH)$_3$(tpy)] (λ_{ex} = 345 nm) complexes in toluene and ethanol.

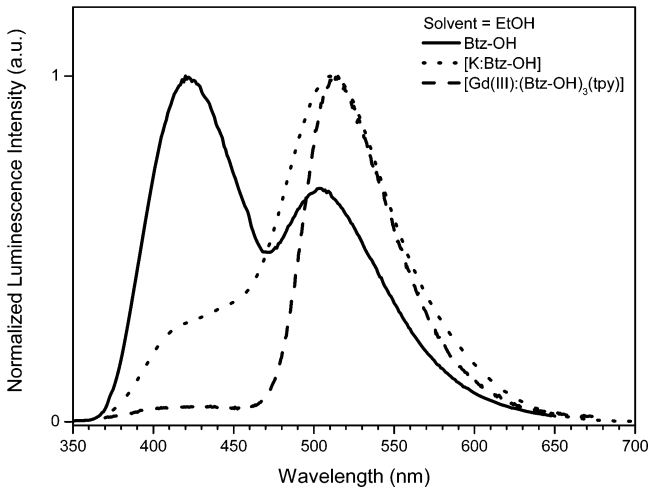

Figure 4. Comparison of luminescence spectra obtained from Btz-OH, [Gd(Btz-OH)$_3$(tpy)], and [Er(Btz-OH)$_3$(tpy)] complexes in ethanol (λ_{ex} = 345 nm).

TABLE 1: Calculated Judd−Ofelt Intensity Parameters of the Nd(III) Ion and [Nd(Btz-R)$_3$(tpy)] Complexes (R = OCH_3 and OH; Units of 10^{-20} cm^2)

material	Ω_2	Ω_4	Ω_6
Nd(III) ion	0.96	4.57	7.17
[Nd(Btz-OCH_3)$_3$(tpy)]	16.12	4.65	8.27
[Nd(Btz-OH)$_3$(tpy)]	18.03	2.90	7.57

$^2G_{7/2}$,$^4G_{5/2}$ transition. As listed in Table 1, the Ω_2 values of the Nd(III) complexes are markedly increased by complexation, compared with those of the free Nd(III) ion. This may be the result of enhanced covalency via the chelation with the ligands. The Ω_λ values of [Nd(Btz-OCH_3)$_3$(tpy)] and [Nd(Btz-OH)$_3$(tpy)] are almost equal, indicating that the stabilities of the two complexes do not differ in the ground state.

Luminescence. Figure 3 shows luminescence spectra of the Ln(III) complexes. The Nd(III), Er(III), and Yb(III) complexes, which were excited at 345 nm for the [Ln(Btz-OCH_3)$_3$(tpy)] complex and 350 nm for the [Ln(Btz-OH)$_3$(tpy)] complex, produced not only visible luminescence but also NIR luminescence. The observed NIR luminescence of the complexes indicates that the energy transfer took place from Btz-R to the Ln(III) ion. The [Gd(Btz-R)$_3$(tpy)] (R = OCH_3 and OH) complexes were also prepared, and their luminescence properties were measured to examine the energy transfer event. As shown in Figure 3, the Gd(III) complexes produced either a strong 420 nm normal emission from Btz-OCH_3 or a strong 550 nm ESIPT emission from Btz-OH. Energy transfer from Btz-R to Gd(III) and the subsequent Gd(III)-centered luminescence did not occur because the energy of the first excited $^6P_{7/2}$ state of Gd(III) is higher than the 345 nm excitation energy. For [Ln(Btz-OCH_3)$_3$-(tpy)], the visible luminescence intensity originating from Btz-OCH_3 was not significantly affected by Ln(III). The slightly reduced intensity of the visible luminescence from the Ln(III) complex producing the NIR luminescence might indicate energy transfer.

The visible emission spectra of the Ln(III) complexes dissolved in ethanol are notably different from those measured from the free Btz-OH. Only the ESIPT emission band appeared in the Gd(III) complex. To prove this difference in spectral distribution, the potassium salts of the Btz-OH ligand, [K(Btz-OH)] were also investigated. As shown in Figure 4, the luminescence spectrum of [K(Btz-OH)] exhibited a typical spectral distribution in ethanol, with the ESIPT band as a main band and the normal band as a minor band. This result suggests that the chelation of a metal ion (K^+ or Ln(III)) with the ligand carboxyl group induces a structural change in the ligand molecule. The complexation of Btz-OH with the metal ion makes the carboxyl moiety negatively charged, which might induce the hydroxyl group to release its proton. This deprotonated group could easily interact with the oxygen atom of the ethanol molecule. Thus, the proton transfer process is achieved indirectly through the ethanol molecule. Accordingly, a red-shifted ESIPT band was also observed in the metal salt of Btz-OH. For [Ln(Btz-OH)$_3$(tpy)], the intensity of the 510 nm ESIPT emission from the Btz-OH moiety varied significantly, depending on which Ln(III) ion is introduced. Thus, energy transfer is more favorable for Btz-OH than for Btz-OCH_3.

For the Yb(III) complexes, the sensitized luminescence with relatively intermediate intensity was observed at 980 nm band. This band is attributed to the transition from the emitting $^2F_{5/2}$ level to the ground $^2F_{7/2}$ level of the Yb(III) ion. For the Nd(III) complexes, three sensitized emission bands appeared, at 880 nm (w), 1060 nm (s), and 1330 nm (w). These bands are attributed to the transitions from the emitting $^4F_{3/2}$ level to the $^4I_{9/2}$, $^4I_{11/2}$, and $^4I_{13/2}$ levels of the Nd(III) ion, respectively. For the Er(III) complexes, a sensitized emission band with relatively weak intensity appeared at 1530 nm, which is attributable to the transition from the emitting $^4I_{13/2}$ level to the ground $^4I_{15/2}$ level of the Er(III) ion. Unexpectedly, when the Er(III) complex was dissolved in ethanol, the characteristic sensitized NIR luminescence appeared as a trace for [Er(Btz-OCH_3)$_3$(tpy)]) or was very weak for [Er(Btz-OH)$_3$(tpy)]. These results indicated a very significant energy loss from the Er(III) complexes, resulting from phonons of the surrounding solvent molecules. Actually, the NIR-emitting levels were seriously influenced by phonons such as C−H or O−H vibrations. The characteristic emission in the NIR region was significantly quenched, as the vibration overtones were well matched to the NIR-emitting level of lanthanide ions. For Er(III), the characteristic luminescence around 1530 nm was almost eliminated by the influence of the phonons provided from ethanol molecules.

Decay Time and Quantum Yield. The NIR luminescence decay profiles were measured upon excitation of the Btz-R (R = OCH_3 and OH) ligand moiety. The 980, 1060, and 1530 nm bands were chosen for monitoring emission wavelengths for Yb(III), Nd(III), and Er(III) complexes, respectively. The measured NIR luminescence decay profiles of the complexes (Figure 5) are well fitted by a single-exponential function. The obtained lifetimes of the sensitized luminescence are listed in Table 2. The quantum yield of the sensitized NIR luminescence of Ln(III) in the complex can be estimated using the following relationship between the experimentally determined lifetime of Ln(III) (τ_{obs}) and its natural lifetime (τ_o):

$$\Phi_{sens} = \frac{\tau_{obs}}{\tau_o} \tag{7}$$

Using reported τ_o values of 2.00 ms for Yb(III), 0.27 ms for Nd(III), and 8.00 ms for Er(III),[37,38] we calculated the quantum yield of the sensitized luminescence (Table 2). The NIR sensitized luminescence quantum yields of the Btz-OH complexes are more efficient than those of the Btz-OCH_3 complexes, indicating that the ESIPT process enhanced the NIR sensitized luminescence. The Nd(III) complexes gave the largest quantum yield, and Er(III) complexes gave the smallest quantum yield.

As described above, a decrease in the intensity of the normal or ESIPT emission from the benzothiazole derivatives is strongly related to the energy transfer process. The sensitized luminescence of Ln(III) results from the excitation of the benzothiazole derivatives into its singlet excited state, energy transfer from the singlet to the resonance level of Ln(III), and the subsequent relaxation to the emitting level. Considering this pathway, the overall quantum yield of the sensitized luminescence can be expressed as

$$\frac{\tau}{\tau_o} = \Phi_{antenna}\Phi_{ET}\Phi_{rel} \tag{8}$$

where the quantum yield of the Gd(III) complex is taken as $\Phi_{antenna}$ and Φ_{rel} is the relaxation efficiency, which is strongly associated with radiationless transition from the receiving level to the emitting level of Ln(III). The energy transfer efficiency

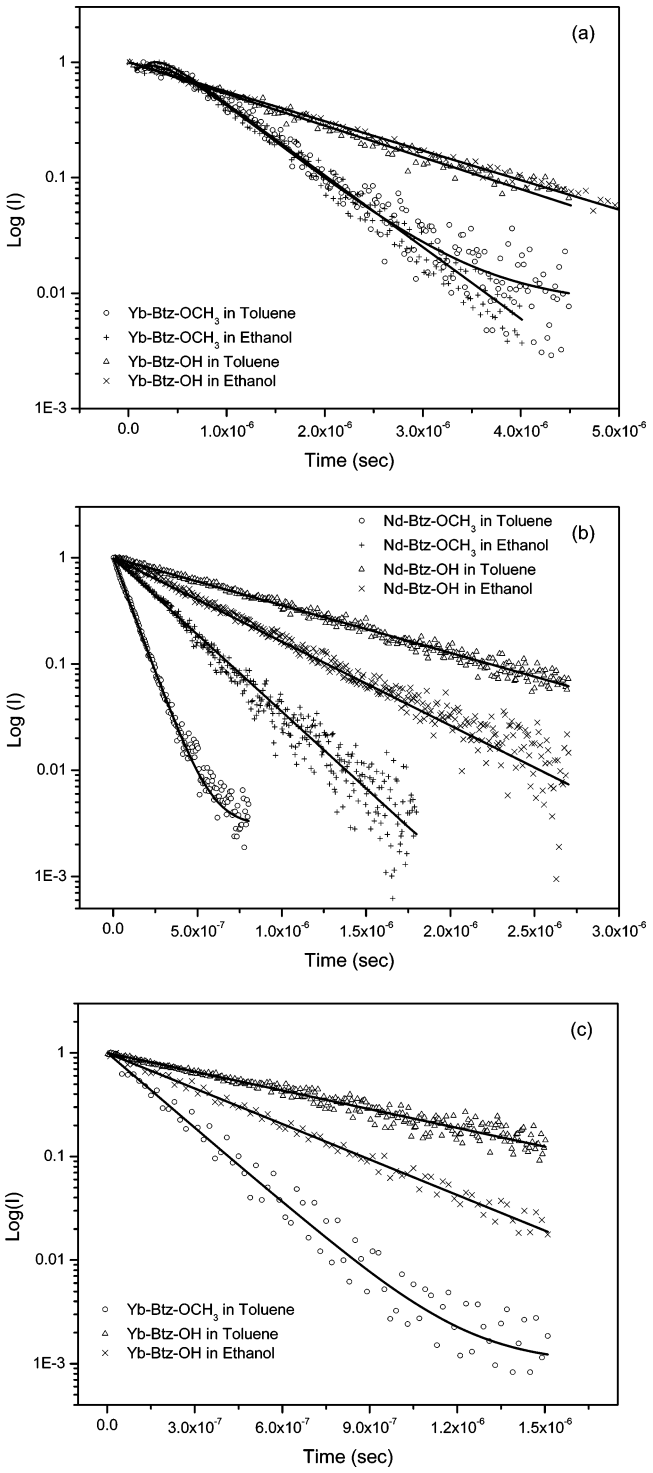

Figure 5. Luminescence decay profiles obtained from [Ln(Btz-R)$_3$(tpy)] complexes in toluene and ethanol (Ln = Yb (a), Nd (b), and Er (c); R = OCH_3 and OH).

(Φ_{ET}) of each lanthanide complex was estimated from a comparison of the peak area between the Gd(III) complex and each NIR-emitting lanthanide complex in the visible region. Substituting the experimentally determined values of $\Phi_{antenna}$ and Φ_{ET} into eq 8, we obtained the Φ_{rel} values. The values listed in Table 2 show that the energy loss during the relaxation was much greater for the Er(III) complexes than for the Yb(III) and Nd(III) complexes. This may be due to the larger energy gap (ΔE) between the energy-donating level of the benzothiazole derivative and the emitting level of the Er(III) ion. The Yb(III) ion has only a single $^2F_{5/2}$ excited state, at 10200 cm^{-1}. As

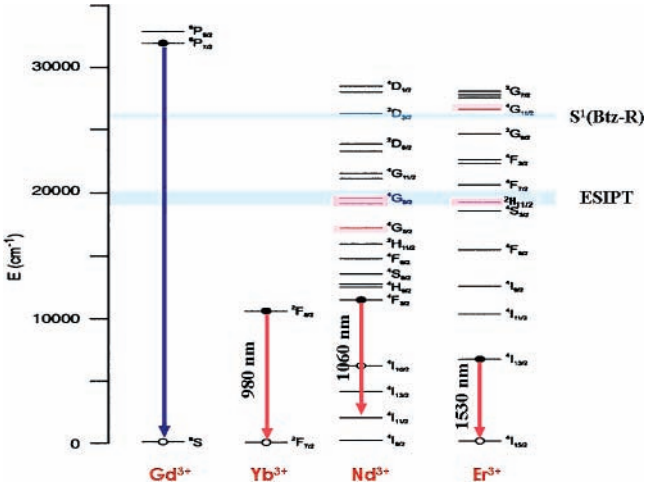

Figure 6. Schematic energy diagram of energy transfer mechanisms in [Ln(Btz-R)$_3$(tpy)] complexes (R = OCH_3 and OH).

TABLE 2: Quantum Yields and Luminescence Lifetimes of [Ln(Btz-R)$_3$(tpy)] Complexes (Ln = Gd, Yb, Nd, and Er; R = OCH_3 and OH)

			quantum yields				
solvents	R	Ln	Φ_{Lig}	Φ_{ET}	Φ_{rel} ($\times10^{-3}$)	Φ_{sens} ($\times10^{-4}$)	τ_{obs} (μs)
toluene	OCH_3	Gd	0.302				
		Yb	0.265	0.122	9.0	3.3	0.65
		Nd	0.208	0.310	4.3	4.0	0.10
		Er	0.236	0.219	0.3	0.2	0.18
	OH	Gd	0.089				
		Yb	0.056	0.370	24.0	7.9	1.58
		Nd	0.009	0.897	48.9	39.0	0.97
		Er	0.020	0.775	1.3	0.9	0.72
ethanol	OCH_3	Gd	0.406				
		Yb	0.392	0.034	25.4	3.5	0.70
		Nd	0.325	0.199	37.1	12.0	0.30
		Er	0.391	0.037			
	OH	Gd	0.078				
		Yb	0.034	0.565	19.3	8.5	1.70
		Nd	0.019	0.760	37.1	22.0	0.55
		Er	0.022	0.716	0.9	0.5	0.38

shown in Figure 6, the energy difference between the $^2F_{5/2}$ level of Yb(III) and the $^4F_{3/2}$ level of Nd(III) is very small. However, the efficiency of Yb(III) is much less than that of Nd(III). This could be related to the fact that Nd(III) has a wealth of accepting levels whereas Yb(III) has only one. This indicates that the energy gap between the energy-donating level of the benzothiazole ligand and the receiving level of Ln(III) plays a key role in the energy transfer process.

Energy Transfer Rate. The energy transfer rate for the sensitized luminescence from an organic ligand to Ln(III) has been explained in terms of their mechanisms for electrostatic interaction and resonance transfer. Previously, we estimated the energy transfer rate for the sensitized NIR luminescence of Er(III) complexes with PtP and tpy ligands using the multipole−dipole and the dipole−dipole mechanisms as the electrostatic interaction.[32] The most significant factors determining the magnitude of the energy transfer rate were the energy mismatching factor ($F \propto e^{-(\Delta E/\hbar\Delta A_L)^2}$) and the selection rule (ΔJ: $J + J' \geq \lambda \geq |J - J'|$, $\lambda = 2$, 4, and 6) between the receiving and the final levels. In F, ΔE is the energy difference between the ligand donor level and the lanthanide ion acceptor level and ΔA_L is the bandwidth at half-height of the ligand state. For the receiving levels satisfying the ΔJ selection rule, the energy transfer from the visible luminescent ligand to the NIR-emitting Er(III) was too small to be accepted. Those results suggest that the resonance energy transfer mechanism is suitable for the NIR-emitting Ln(III) complex in the solution state.

TABLE 3: Calculated Critical Radius (R_0) and the Expected Energy Transfer Rate Constants (k_{et}) of the Ln(III) Complexes

solvent	R	Ln	R_0 (Å)	k_{et} (10^9 s^{-1})
toluene	OCH_3	Nd	10.44	1.08
		Er	10.24	0.96
	OH	Nd	12.95	4.54
		Er	11.54	2.69
ethanol	OCH_3	Nd	11.25	1.69
		Er	10.97	1.46
	OH	Nd	13.09	5.72
		Er	11.97	3.36

We estimated the energy transfer rate using the energy transfer mechanism described by eq 4. In eq 4, the actual donor−acceptor distance, R_L, was calculated by theoretical geometry optimization (molecular mechanics MM+ method), resulting in a distance of approximately 8.84 Å. All possible levels of Ln(III), the absorption band of which overlapped with the normal and the ESIPT bands of Btz-R were considered in the calculation. The calculated resonance energy transfer rates of [Ln(Btz-R)(tpy)] (Ln = Nd and Er) dissolved in organic solvents are listed in Table 3. The energy transfer rates of Btz-OH to Nd(III) and Er(III) are greater than those for the Btz-OCH_3 complexes. Figure 6 shows an energy diagram, including a comparison between the f−f transition level of the lanthanide ions and the ligand luminescence level. The hypersensitive f−f transition levels of lanthanide ions are $^4G_{5/2}$ for Nd(III) and $^2H_{11/2}$ for Er(III). Figure 6 illustrates that the ligand levels were moved toward the hypersensitive levels of lanthanide ions due to ESIPT, which increased the spectral overlap integral between the ligand emission band and the hypersensitive absorption band of Ln(III). In toluene, the weight of the transferred energy to the nearly degenerate $^4G_{7/2}$ and $^2G_{7/2}$ states of Nd(III) is only 9% for the Btz-OCH_3 complex, but it increased to 30% for the Btz-OH complex. Similarly, the weight of the transferred energy to the $^2H_{11/2}$ state of Er(III) was increased from 15% to 39% by ESIPT. In addition, the energy gap between the emission level of the ligand and the emitting level of the lanthanide ion was decreased, which also contributed to the enhancement of the sensitized NIR luminescence quantum yields by decreasing the energy loss through radiationless transition.

Conclusion

This study revealed that lanthanide complexes containing Btz-R (R = OCH_3 and OH) and tpy can produce sensitized NIR luminescence by energy transfer from Btz-R to Ln(III). The Btz-OH ligand dissolved in toluene undergoes ESIPT, leading to a red shift in the luminescence spectrum. The change in the spectral distribution of the ligand molecule increased the spectral overlap integral between the luminescence band of the ligand and the hypersensitive absorption bands of Nd(III) and Er(III), thus enhancing the quantum yield of the sensitized NIR luminescence. The quantum yield of the Nd(III) complex was more efficient than that of the Er(III) complex, due to the smaller energy gap between the emitting and ground levels of Er(III). Theoretical calculation confirmed that the Förster resonance energy transfer mechanism correctly explained the energy transfer constants of $\sim10^9$ s^{-1} for the NIR-emitting Ln(III) complexes.

Acknowledgment. This work was financially supported by the Korean Ministry of Science and Technology through the

National Research Laboratory Program at Hannam University. M.-K.N. and J.-G.K. acknowledge financial support from Alti-electronics Co.

References and Notes

(1) Mears, R. J.; Baker, S. R. *Opt. Quantum Electron.* **1992**, *24*, 517.
(2) Kim. H. K.; Roh, S. G.; Hong, K.-S.; Ka, J.-W.; Baek, N. S.; Oh, J.-B.; Nah, M.-K.; Cha, Y.-H.; Ko, J. *Macromol. Res.* **2003**, *11*, 133.
(3) Wolbers, M. P. O.; van Veggel, F. C. J. M.; Peters, F. G. A.; van Beelen, E. S. E.; Hofstraat, J. W.; Guerts, F. A. J.; Reinhoudt, D. N. *Chem.—Eur. J.* **1998**, *4*, 772.
(4) Lis, S.; Elbanowski, M.; M_kowska B.; Hnatejko, Z. *J. Photochem. Photobiol., A* **2002**, *150*, 233.
(5) Quici, S.; Cavazzlini, M.; Accorsi, G.; Armaroli, N.; Ventura, B.; Barigelletti, F. *Inorg. Chem.* **2005**, *44*, 529.
(6) Kang, J.-G.; Kim, T.-J.; Kang, H.-J.; Kang, S. K. *J. Photochem. Photobiol., A* **2005**, *174*, 28.
(7) Sun, L.-N.; Zhang, H.-J.; Peng, C.-Y.; Yu, J.-B.; Meng, Q.-G.; Fu, L.-S.; Liu, F.-Y.; Guo, X.-M. *J. Phys. Chem. B* **2006**, *110*, 7249.
(8) Lazarides, T.; Alamiry, M. A. H.; Adams, A.; Pope, S. J. A.; Faulkner, S.; Weinstein, J. A.; Ward, M. D. *Dalton Trans.* **2007**, *15*, 1484.
(9) Baek, N. S.; Kim, Y. H.; Roh, S.-G.; Kwak, B. K.; Kim. H. K. *Adv. Funct. Mater.* **2006**, *16*, 1873.
(10) Nah, M.-K.; Cho, H.-K.; Kwon, H.-J.; Kim, Y.-J.; Park, C.; Kim, H. K.; Kang, J.-G. *J. Phys. Chem A* **2006**, *110*, 10371.
(11) Wolvers, M. P. O.; van Veggel, F. C. J. M.; Snellink-Ruel, B. H. M.; Hofstraat, J. W.; Guerts, F. A. J.; Reinhoudt, D. N. *J. Chem. Soc., Perkin Trans.* **1998**, *10*, 2141.
(12) Steemers, F. J.; Verboom, W.; Reinhoudt, D. N.; van der Tol, E. B.; Verhoeven, J. W. *J. Am. Chem. Soc.* **1995**, *117*, 9408.
(13) Neogi, S.; Savitha, G.; Bharadwaj, P. K. *Inorg. Chem.* **2004**, *43*, 3771.
(14) Zhang, J.; Badger, P. D.; Geib, S. J.; Petoud, S. *Angew. Chem., Int. Ed.* **2005**, *44*, 2508.
(15) Comby, S.; Imbert, D.; Chauvin, A.-S.; Bünzli, J.-C. G. *Inorg. Chem.* **2006**, *45*, 732.
(16) Kuila, D.; Kwakovszky, G.; Murphy, M. A.; Vicare, R.; Rood, M. H.; Fritch, K. A.; Fritch, J. R. *Chem. Matter.* **1999**, *11*, 109.
(17) Unzhinov, B. M.; Druzhinin, S. I. *Russ. Chem. Rev.* **1998**, *67*, 123.
(18) Rodembusch, F. S.; da Silveira, N. P.; Samios D.; Campo, L. F.; Stefani, V. *Mol. Cryst. Liq. Cryst.* **2002**, *374*, 367.
(19) Rodembusch, F. S.; da Silveira, N. P.; Samios D.; Campo, L. F.; Stefani, V. *J. Polym. Sci., Part B: Polym. Phys.* **2003**, *41*, 341.
(20) Holler, M. G.; Campo L. F.; Brandelli, A.; Stefani, V. *J. Photochem. Photobiol., A* **2002**, *149*, 217.
(21) Ireland, J. F.; Wyatt, P. A. H. *Adv. Phys. Org. Chem.* **1976**, *12*, 131.
(22) Kasha, M.; McMorrow, D. *J. Am. Chem. Soc.* **1983**, *105*, 5133.
(23) Das, K.; Sarkar, N.; Gosh, A. K.; Majumdar, D.; Nath, D. N.; Bhattacharyya, K. *J. Phys. Chem.* **1994**, *98*, 9126.
(24) Zapotoczny, S.; Danel, A.; Sterzel, M. T.; Pilch, M. *J. Phys. Chem. A* **2007**, *111*, 5408.
(25) Demas, J. N.; Crosby, G. A. *J. Phys. Chem.* **1971**, *75*, 991.
(26) Judd, B. R. *Phys. Rev.* **1962**, *127*, 750.
(27) Ofelt, G. S. *J. Chem. Phys.* **1962**, *37*, 511.
(28) Carnall, W. T.; Fields, P. R.; Rajnak, K. *J. Chem. Phys.* **1968**, *49*, 4424.
(29) Carnall, W. T.; Fields, P. R.; Wybourne, B. G. *J. Chem. Phys.* **1965**, *42*, 3797.
(30) Weber, M. J. *Phys. Rev.* **1967**, *157*, 262.
(31) Ebendorff-Heidepriem, H.; Ehrt, D.; Bettinelli, M.; Speghini, A. *J. Non-Cryst. Solids* **1998**, *240*, 66.
(32) Nah, M.-K.; Oh, J. B.; Kim, H. K.; Choi, K.-H.; Kim, Y.-R.; Kang, J.-G. *J. Phys. Chem. A* **2007**, *111*, 6157.
(33) Lakovicz, J. R. *Principles of Fluorescence Spectroscopy*, 2nd ed.; Kluwer Academic/Plenum Publishers: New York, 1999.
(34) de Vivie-Riedle, R.; De Waele, V.; Kurtz, L.; Riedle, E. *J. Phys. Chem. A* **2003**, *107*, 10591.
(35) Henary, M. M.; Fahrni, C. J. *J. Phys. Chem. A* **2002**, *106*, 5210.
(36) Mosquera, M.; Penedo, J. C.; Rodríguez, M. C. R.; Rodríguez-Prieto, F. *J. Phys. Chem.* **1996**, *100*, 5398.
(37) Weber, M. J. *Phys. Rev.* **1968**, *171*, 283.
(38) Hofstaat, J. W.; Oude Wolbers, M. P.; Van Veggel, F. C. J. M.; Reinhoudt, D. N.; Werts, M. H. V.; Verhoeven, J. W. *J. Fluoresc.* **1998**, *8*, 301.